

# Estimation of the snow water equivalent using Muon Scattering Radiography

Aitor Orio-Alonso<sup>1,3</sup>, Esteban Alonso-González<sup>2</sup>, Carlos Díez-González<sup>1</sup>, and Pablo Gómez-García<sup>1</sup>, Pablo Martínez-Ruiz del Árbol<sup>3</sup>

<sup>1</sup>Muon Tomography Systems S.L - Bilbao, Spain.

<sup>2</sup>Centre d'Etudes Spatiales de la Biosphère (CESBIO) - Université de Toulouse, CNRS/CNES/IRD/INRA/UPS - Toulouse, France.

<sup>3</sup>Instituto de Física de Cantabria (IFCA) - UC-CSIC - Santander, Spain.

Corresponding author: Pablo Martínez Ruiz del Árbol ([parbol@ifca.unican.es](mailto:parbol@ifca.unican.es))

## Key Points:

- We test the suitability of Muon Scattering Radiography to infer the Snow Water Equivalent.
- Numerical simulations show the technique can estimate the Snow Water Equivalent with a precision of around 1 cm.
- Laboratory measurements confirm the results obtained with simulation.

## Abstract

Despite the important hydrological and ecological implications of the snowpack, its real time monitoring remains challenging. This is particularly relevant in relation to the *Snow Water Equivalent* (SWE), as the available technologies which measure it, exhibit a number of limitations that difficult their operational implementation. In this work, we explore the potential of a new technology, *Muon Scattering Radiography* (MSR), to infer the SWE. We coupled snowpack simulations generated by the SNOWPACK model, with a muon scattering simulation program based on GEANT4. The SWE is modelled as a function of the muon scattering distributions. Predictions of the SWE along the year are provided showing a *root-mean-square error* (RMSE) of 12 mm for 5 hour continuous measurements. We also performed laboratory measurements using ice samples, confirming the SWE estimation capabilities and the potential of the technique to operate as a SWE monitoring tool.

## Plain Language Summary

The monitoring of the seasonal snowpack is important to understand and predict the dynamics of the hydrological and ecological processes, but its continuous monitoring is still a scientific challenge. Particularly in relation to the *Snow Water Equivalent* (SWE), which represents the depth of water that would result if the snow melted. The available technologies to monitor the SWE exhibit a number of limitations that prevent its use in many real world cases. Here we explore the potential of a new technology, *Muon Scattering Radiography* (MSR), to quantify the SWE. MSR is a technique based in the detection of the natural and innocuous radiation of muon particles. The technique consists in the measurement of muon deviations, which depend on the material they traverse. The larger or denser the material is, the bigger the deviations they undergo. This study begins with a detailed simulation. Firstly, we simulated the snowpack evolution itself, and secondly its measurement process. Thirdly, we determined the relation between muon deviations and SWE. And finally, we estimated the precision in the determination of SWE comparing the predictions to the ground truth in the simulations. The results yielded a precision of about 1 cm. We also performed laboratory measurements with ice samples, using a 4 layer muon detector based on multiwire proportional chambers and confirming the potential of the technique to operate as a SWE monitoring tool.

## 1 Introduction

The seasonal snowpack plays a key role in the hydrology of the areas where it is present and beyond (Barnett et al., 2005), but its real-time monitoring still represents a big challenge for the scientific community and water management agencies. Real-time monitoring systems strongly rely on remote sensing and numerical modelling. However, to date, there is still no effective approach to retrieving the snow water equivalent (SWE) from orbital sensors, especially over complex terrain (Luo et al., 2021). In addition, even the most sophisticated physically based snowpack models suffer from the limitations of the quality of the forcing (Raleigh et al., 2016), its parametrizations (Günther et al., 2019), and the uncertainty caused by the wind and avalanche snow redistribution (Vionnet et al., 2021).

Direct observations of the snowpack are very appreciated for water management purposes, long-term climatological studies, as well as for model and remote sensing product validation or data assimilation. However, as a consequence of the difficulties of snowpack monitoring and increased costs, the available SWE time series are often scarce, incomplete, or just inexistent (Alonso-González et al., 2018). In addition, despite nowadays it is possible to retrieve the snow depth using relatively cost-effective techniques (Revuelto et al., 2021), the monitoring of the SWE remains elusive.

Traditional SWE monitoring techniques including snow pillows exhibit a number of limitations that prevents their usage for many applications and environmental conditions. Their installation requires very complex logistics and additionally, these devices often require manual recalibrations (Moreno et al., 2010). Moreover, their accuracy is very limited in ephemeral or shallow snowpacks. In this context, the use of cosmic-ray neutron-based sensors is not uncommon, being the solution chosen by several water agencies for their operational networks. It is possible to deploy neutron-based monitoring networks, even in mountainous or remote regions (Jitnikovitch et al., 2021). However, its precision is still limited and requires a proper in-situ calibration. Despite the relative success of neutron-based techniques, there is still a need for scientific innovation in the field of SWE sensors.

Muons are leptons, elementary particles similar to electrons but with a mass about 207 times greater. Cosmic rays, very high-energy particles and nuclei that constantly reach the earth from deep space, collide with the upper layers of the atmosphere producing a shower of several types of secondary particles. Some of them manage to reach the sea level, indeed, muons are the most numerous charged particles at this atmospheric depth (Workman et al. (Particle Data Group), 2022).

Thus, cosmic muon production is a very common natural phenomenon. Muons exhibit high penetrating capabilities, being interesting candidates for the development of SWE sensors. Although they have great potential, their option as a resource to measure the SWE is largely underexplored yet. Consequently, there is a lot of room for research and development in this field.

There are two different types of muography: *Muon Absorption Radiography* (MAR), a technique that uses muon counts to extract information, and *Muon Scattering Radiography* (MSR), which utilises muon deviations. Recently, Gugerli et al. (2021), applied MAR and proved the potential of muon counters to infer the SWE in the field, comparing the decreasing muon count rate with in situ SWE measurements.

The objectives of this study are: (1) to infer SWE by conducting a detailed study using snowpack and a detailed muon numerical simulation and (2) to test the capabilities of a real-world hardware designed by us to measure SWE contained in artificial snow samples.

## 2 Materials and Methods

### 2.1 Physical principle

Muons, being a charged particle, suffer many small-angle scatters when traversing matter. Most of this deflection is due to Coulomb scattering with nuclei of matter, as described by the Rutherford cross section. The multiple scattering phenomenon can be described through the theory of Molière. Although large scatters produce a non-Gaussian tail in the probability distribution of the total deviation of muons when traversing a certain material, it can be approximated by a Gaussian distribution with a RMS width ( $\theta_0$ ) of (Workman et al., 2022; see also Bethe, 1953; Highland, 1975; Lynch et al., 1991):

$$\theta_0 = \frac{13.6 \text{ (MeV)}}{\beta p} \sqrt{\frac{x}{X_0}} \left[ 1 + 0.038 \ln\left(\frac{x}{X_0 \beta^2}\right) \right] \quad (1)$$

Where  $p$  and  $\beta c$  are the momentum and velocity of the incident particle.  $x$  is the distance traversed by the particle inside the material and  $X_0$  is the radiation length of the material.  $\beta$  represents the ratio between the particle velocity and the speed of light. The constant 13.6, is measured in millions of electronvolts (MeV) and  $\theta_0$  represents the RMS value of muon deviations projected in a plane.

### 2.2 Experimental setup

Muon data used in this work has been collected with our muon detection system (Figure 2, b). This muon monitoring system is currently in use for both scientific and industrial purposes (Martínez-Ruiz del Árbol et al., 2022). The particle detectors are composed of four Multi-Wire Proportional Chambers (MWPC) and each chamber has two layers with 224 detection wires, all of them separated by 4 mm. The two layers form a two-dimensional grid of wires which covers an area of 89.6 x 89.6 cm and detects the positions where muons cross it.

The synchronisation electronics identify a muon when signals are obtained in a space of time on the order of hundreds of microseconds in all the chambers, in both the upper and lower detector. This condition distinguishes signals produced by muons from signals produced by other charged particles which could activate detection wires, since this kind of simultaneous activations on the earth's surface are practically only produced by muons. However, various sources of noise should be considered, such as charged hadrons, electrons, and positrons (“fake muons”), and also muons with relatively low momentum (“soft muons”) (Bonechi et al., 2020).

When a muon event is identified, our system detects four points located in the horizontal two-dimensional grids, two points before the particle goes through the target and another two points after the particle traverses it. With this data, way-in and way-out trajectories can be reconstructed, and muon deviations calculated. Specifically, in the numerical analysis of this

work, we utilised the projection of muon deviations in two planes perpendicular to the detection wires, in agreement with the deviations represented by  $\square_0$  in the Equation 1.

### 2.3 Simulation setup

The snowpack was simulated using a one-dimensional snow model forced by surface meteorological data. We have used the SNOWPACK model (Bartelt & Lehning, 2002; Lehning et al., 2002a; Lehning et al., 2002b) to realistically simulate the behaviour of the snowpack along two seasons, 2015/2016 and 2016/2017 (Figure 1). SNOWPACK is a physically-based multilayer model that simulates the state and microstructure of the snowpack. It is based on the energy and mass balance of the snow, and it is widely used for both research and operational snow avalanche forecasts. For this study, SNOWPACK was forced by the ERA5-Land surface reanalysis (Muñoz-Sabater et al., 2021). The simulations were performed in the Pyrenees, using the ERA5-Land cell whose centroid falls closer to the Monte Perdido massif (42.7°N, -0.1°E), at an elevation of 2041m asl. The main objective of these simulations was to generate detailed snowpack state variables that realistically evolve along the time dimension, providing information on the different conditions in both accumulation and melting periods, as well as its internal structural characteristics. Once the SNOWPACK simulations were performed, we retrieved from them the ice, liquid water, and air content of each variable height snow layer which constitutes the whole sample, as well as the bulk density and the total snow depth.

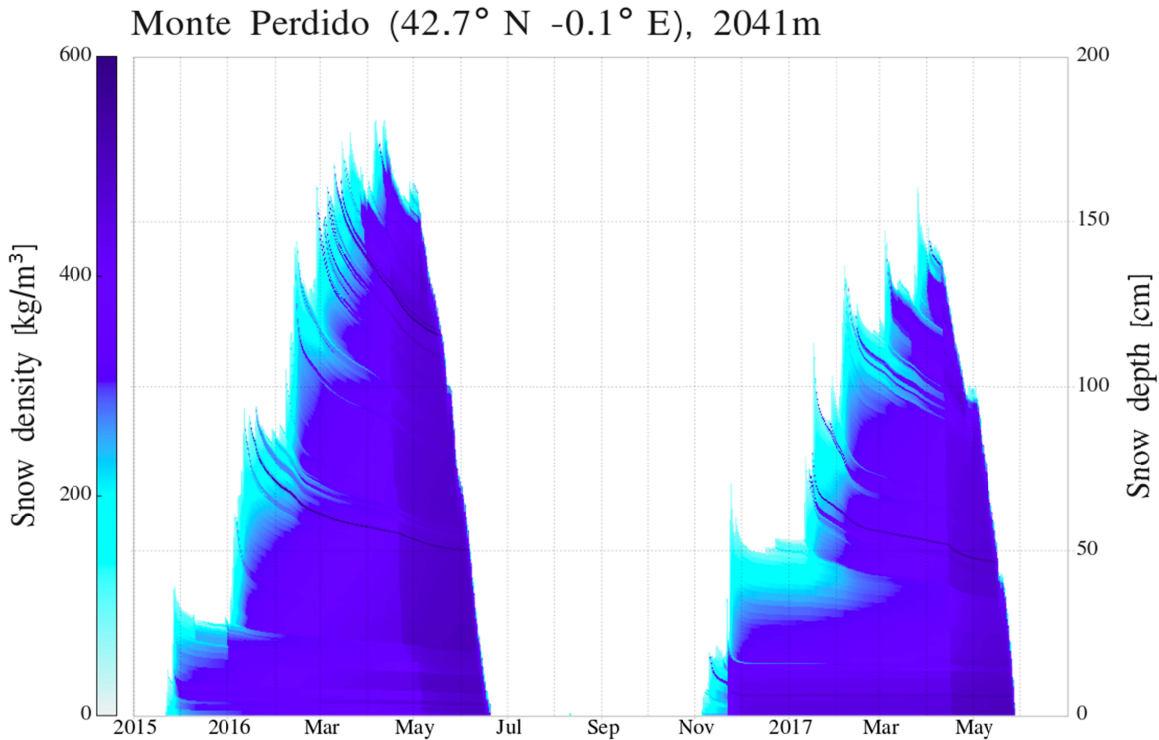


**Figure 1.** Snowpack density and depth time evolution during 2015/2016 and 2016/2017 hydrological years simulated with SNOWPACK model forced by ERA5-Land.

189

190 We coupled the SNOWPACK simulations with a full MSR simulation setup that uses the  
 191 Cosmic Ray generator (Hagmann et al., 2012) to reproduce the atmosphere muon flux and  
 192 GEANT4 (Agostinelli et al., 2003) to simulate the muon scattering caused by the snowpack  
 193 (Figure 2, a). GEANT4 is a state-of-the-art software designed and maintained at CERN to  
 194 simulate the interactions of particles and matter in high-energy and nuclear physics. Our  
 195 simulation framework contains a model of our experimental setup including the muon detectors  
 196 and their response. This framework has been successfully applied to multiple industrial  
 197 problems, for instance, to steel-made pipe wear (Martínez-Ruiz del Árbol et al., 2018). Similar  
 198 simulation frameworks are typically used to research applications of muography (Mori et al.,  
 199 2017).

200 Once the numerical SNOWPACK simulations were developed, we expanded the one-  
 201 dimensional snowpack geometry to a 1m<sup>2</sup> snow column, assuming homogeneous snow layers in  
 202 the longitude and latitude dimensions. Then, we propagated and measured muons penetrating the  
 203 whole snow column, virtually reproducing the detection process using GEANT4 and collecting  
 204  $\square_0$  for different accumulations of snow during the two simulated seasons.

#### 205 2.4 Measurements and analysis strategy:

206

207 The detection angular resolution is a key parameter in MSR application. This resolution refers to  
 208 the smallest muon angular deviation measurable by the detectors, and it is determined by the  
 209 separation of the wires within detection layers, the separation of the chambers of each trajectory  
 210 detector (in this case, upper detector, and lower detector) and the materials of the detectors  
 211 themselves, which inevitably produce an intrinsic angular deviation of the muons. The resolution  
 212 strongly impacts the final performance of the technique and it is of great importance for this  
 213 work, where the target object is composed of a low density material such as snow.

214

215 To demonstrate the capability to infer the SWE and to explore the previously commented  
 216 influence of detector resolution and of their material itself, we analysed MSR data produced in  
 217 different scenarios. We built 4 simulation scenarios to study in detail the changes induced by the  
 218 factors affecting the resolution. The first scenario considers muon detectors with a perfect spatial  
 219 resolution and neglecting the effect of the detector materials. In the second scenario, the effect of  
 220 the detector materials is simulated but still assuming a perfect spatial resolution. In the third  
 221 scenario, detector materials are considered and the spatial resolution is degraded by setting the  
 222 wire separation to 4 mm. All these scenarios assume a detector layer separation of 257 mm. The  
 223 fourth scenario is similar to the previous but assuming a detector layer separation of 130 mm,  
 224 coincident with the experimental setup. In each of these scenarios we quantify the correlation  
 225 between measured muon deviations and SWE. Finally, we made laboratory measurements on  
 226 blocks of ice of different heights, to test the performance of our hardware and confirm the  
 227 simulation results.

228

For each type of simulation (scenarios 1, 2, 3, 4), we analysed weekly measurements of 5 hours during the first snowing season, the hydrologic year 2015/2016 (Figure 1). These simulations were used to model the relation between  $\theta_0$  and SWE in different conditions. With this data we wanted to study the influence of the spatial resolution of the detection wires, of the chamber separation, and of the detector material itself. Finally, we produced additional data with the realistic resolution and all the other simulation settings of scenario 3, to use it for validation. We simulated the measurement of the whole hydrologic year 2016/2017, gathering continuous 5-hour measurements.

We used our laboratory setup to measure the SWE of artificial snow samples of known density and volume. The samples were composed of crushed slices of ice, emulating real snow (Figure 2, c). The first one consisted of an empty container, and it was used as a reference to measure the intrinsic  $\theta_0$  observed in our setup. In the second, we introduced 10.60 Kg of material with a bulk density of 448.70 Kg/m<sup>3</sup>, reaching a height of approximately 22.3 cm in the container and 99.8 mm of SWE. Finally, in the third sample, we used 21.20 Kg of material with a bulk density of 494.92 Kg/m<sup>3</sup>, reaching 40 cm and summing 197.97 mm of SWE. We performed a single 5-hour measurement, for each sample.

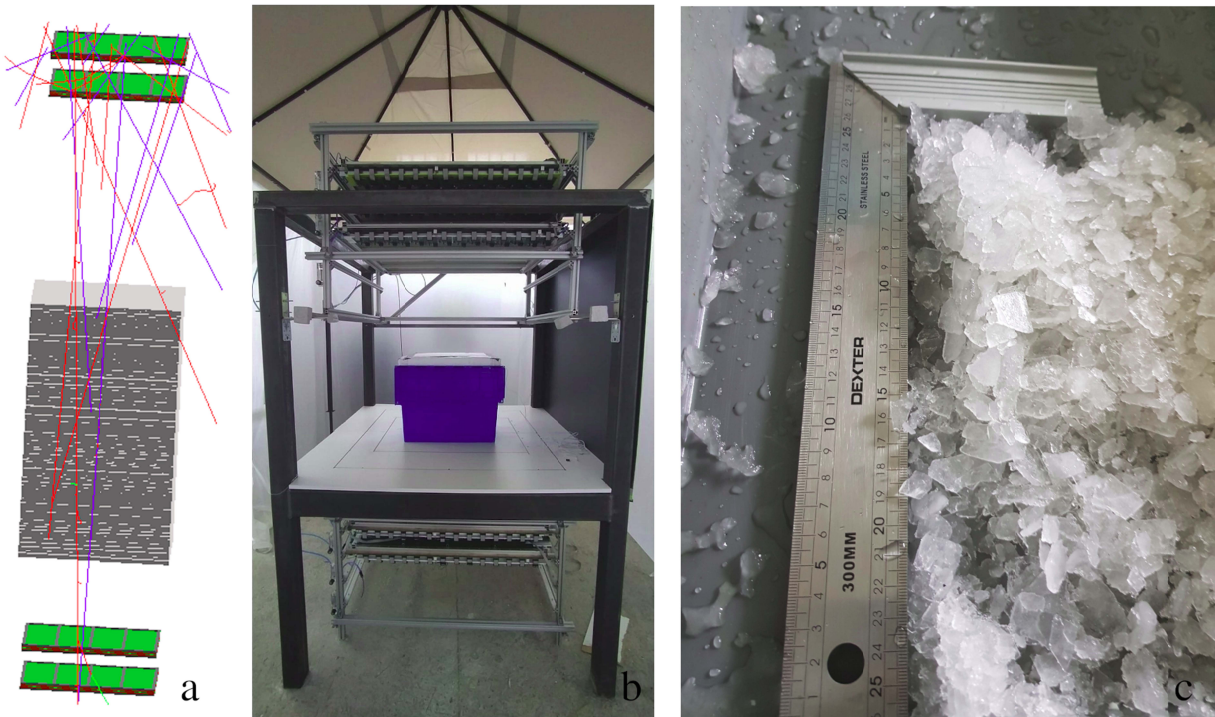


**Figure 2.** Experimental setups. (a) Simulation scenario with the virtual copy of the hardware, a snow sample and representation of particle propagation. (b) The hardware, with a snow sample placed between the detectors. (c) Detail of the crushed ice used to emulate the composition of the snow.

A simple mathematical model has been developed in order to connect the SWE with the standard deviation of the muon angular deviations. This model considers a constant term to account for the intrinsic resolution due to all the instrumental effects, and a term proportional to the square root of the SWE. The second term assumes that the SWE is proportional to the number of radiation lengths of the target, according to equation 2.

$$\theta_0 = p_0 + p_1 \sqrt{SWE} \quad (2)$$

We fitted Equation 2 to all scenarios, expecting to obtain different fit parameters  $p_0$  and  $p_1$  for each of them, since different detector conditions are being considered.

### 3 Results

We modelled  $\theta_0$  for different scenarios of simulated and real snow samples as a function of the SWE using Equation 2. Figure 3 shows the results for all the scenarios including its fitted function. For this analysis, we rejected muons with projected deviations higher than 100 mrad, with the aim of reducing the previously mentioned sources of noise, namely, “fake muons” and “soft muons”. As expected, the observed data is compatible with a root square function. In all the scenarios the coefficient of determination between the two variables is around 0.98. Only a slight decrease is noticed in the case of scenario 2, the one with 4 mm wire separation and 13 cm chamber separation. All the models fit to the expected square root relation, but each one has different fit parameters  $p_0$ , and  $p_1$ . There is a bias at 0 mm of SWE ( $p_0$  variation), and also different intensity in the increment of the measured variable in relation to the SWE ( $p_1$  variation) depending on the scenario. These preliminary results clearly show the increase produced in  $\theta_0$  when detector material is considered, and when detector resolution is diminished. The  $\theta_0$  increase due to detector material significantly decreases in agreement with the SWE increment, while the  $\theta_0$  increase produced by the detector resolution is present in all the simulated SWE range.

In the results obtained with the two setups with perfect resolution (scenarios 1 and 2), an increase of  $\theta_0$  due to detector material can be observed, which is more noticeable at lower SWE measurements. The scenarios 2 and 3 show a  $\theta_0$  increase produced by the limited resolution of the detection wires. Furthermore, between the scenarios 3 and 4, a  $\theta_0$  increase produced by the change of detector separation appears. And finally, the laboratory measurements show higher  $\theta_0$  values. The main differences between our laboratory setup and the simulation scenario 4 are the precision of the alignment of the detectors, the presence of an additional steel-made structure, noise and effects not considered in simulation, and the snow samples themselves. Some of these factors are probably responsible of the higher  $\theta_0$  values obtained in our laboratory. It also has to

be mentioned that the laboratory measurements were performed inside a building which was not included in simulation.

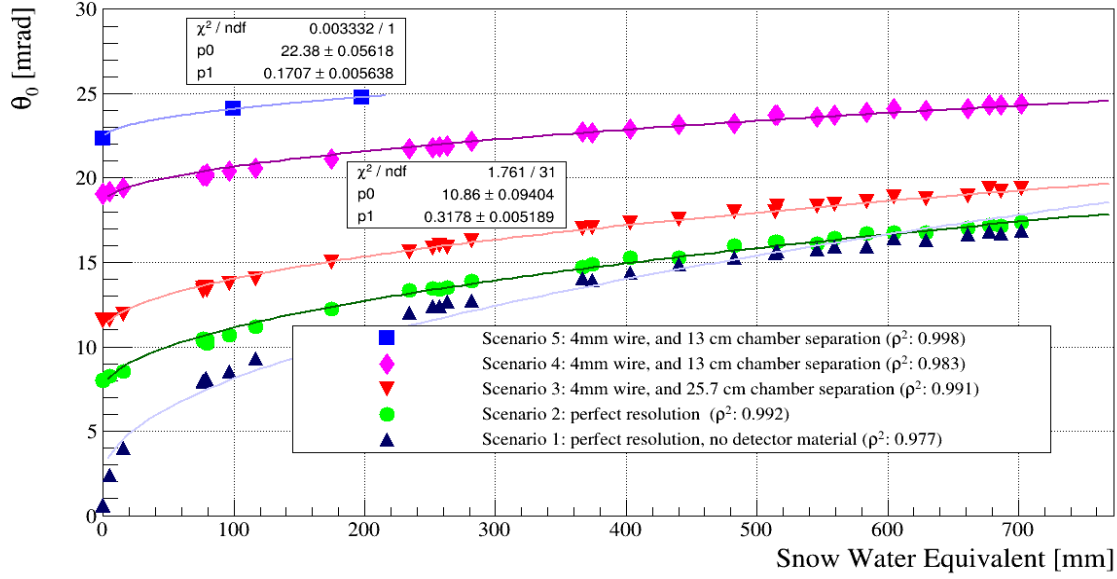


**Figure 3.** RMS of the muon scattering angles as a function of SWE for different scenarios. The laboratory setup or scenario 5, and the simulated cases: scenarios 4, 3, 2, and 1.

In order to calculate the SWE of additional and independent snowpack samples, we extracted a SWE estimation function for the scenario 3 from its fitted model (Figure 3):

$$SWE_{\mu} = \left( \frac{\theta_0 - (10.86 \pm 0.09)}{(0.318 \pm 0.005)} \right)^2 \quad (3)$$

Where  $SWE_{\mu}$  is the SWE estimation made by means of MSR for an individual measurement, and  $\theta_0$  is the RMS value of the measured muon deviations during the same measurement. To validate the defined function, we applied the SWE estimation formula to independent measurements of snow samples. For that purpose, we used the second season data (hydrologic year 2016/2017), obtaining results that show a RMSE of 11.5 mm, tending to underestimate (overestimate) the SWE during the minimum (maximum) accumulation periods (Figure 4). We obtained an average underestimation of 9.4% (14.3 mm SWE) for the month of december, while average overestimation during april was 3.3% (15.7 mm SWE).

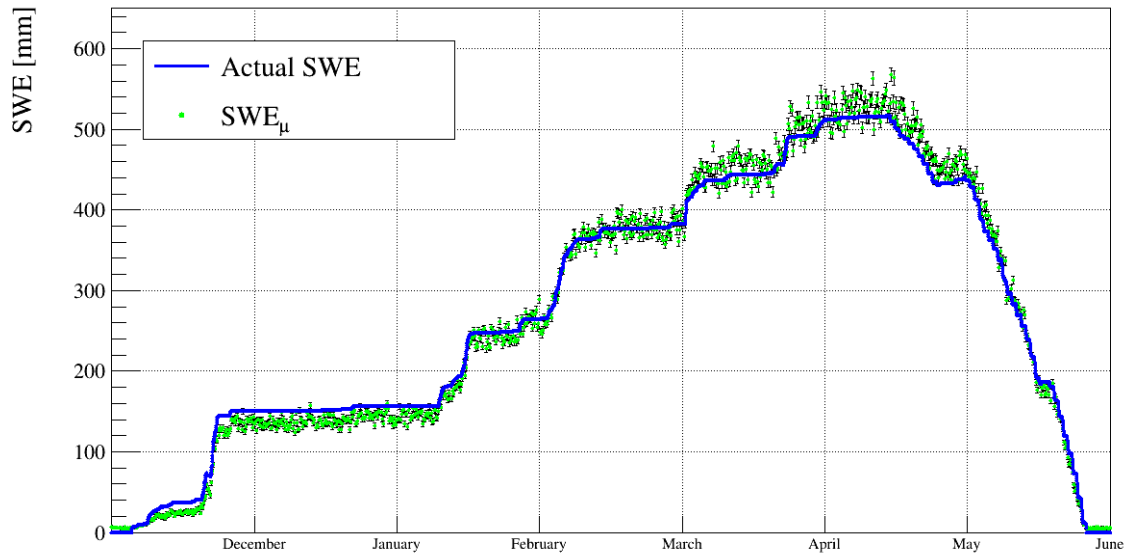


**Figure 4.** Validation of the SWE estimation function with data of the season 2016/2017 (scenario 3). The green dots are the results of the SWE estimation function ( $SWE_{\mu}$ ), while the blue line indicates the actual SWE. The black bars represent the uncertainty of the model, based on the propagation of the fitted parameter variance. In the horizontal axis, the beginning of each month is signalled.

#### 4 Discussion and Conclusions

In this work we demonstrated that MSR can be used to determine the SWE, and therefore, it could be a viable technology to help solve the existing challenges in the real time monitoring of the snowpack.

We have developed snowpack simulations and built and validated a simulation numerical model which identifies the relation between muon deviations and SWE. The theoretical reference represented by the Equation 1, and also previous studies analysing similar relations (Zeng et al., 2020) agree with our results. In addition, the simulation model is compatible with the three snowpack measurements performed in the laboratory, proving the agreement of our simulations with reality. The higher  $\theta_0$  obtained in the laboratory measurements, can be explained by the presence of the steel-made detection structure (Figure 2, b), and by millimetre scale misalignments of the detector chambers, noise and other effects of the detection process that could be minimised in specific designs. The mentioned factors are not included in the simulations, and they make the muons undergo higher deviations. The uncertainty created by the probable differences between simulation and laboratory muon flux and momentum spectrum, should be also considered. The laboratory measurements were performed inside a building, and this fact could produce significant changes on muon flux and momentum compared to the

simulations, which do not include the building effect. The different characteristics of the artificial snow sample and the simulated snow, such as the analysed surface and their material, are a source of uncertainty as well. But in spite of the mentioned subtle disagreements and uncertainties, the achieved compatibility is a very promising point regarding the possibility of using simulation data for SWE detection modelling, calibration and testing.

Although the agreement of data extracted from different scenarios matched our expectations, we performed additional studies about the influence of different factors that affect our SWE modelling procedure, such as detector resolution and their own material. The resolution modifies how we detect muon deviations, and as in these experiments the majority of muons undergo deviations on the order of tens of milliradians, when the resolution gets worse, the measured deviations increase significantly. On the other hand, the detector material increases the actual scattering that muons undergo. And both, detector resolution and material, influence the relation between the measured deviations and the SWE. Therefore, a specific modelling is required depending on the detection setup. But above all, it is remarkable that in all the measurement scenarios the coefficient of determination between the two variables is 0.98 or higher. In relation to the measurements performed in the laboratory with our hardware, it is desirable to continue exploring the potential of MSR and to test the technique in the field.

We also validated the simulation numerical model evaluating its estimates for additional and independent continuous measurements during the hydrologic year (2016/2017). The evaluation yielded successful SWE estimations, with an average RMSE of 11.5 mm for the whole year. This last validation demonstrates the ability of the technique to continuously monitor the SWE using a model built with weekly measurements made during a unique season.

Gugerli et al. (2021) already demonstrated the SWE monitoring capability of MAR, measuring in the field the muon attenuation and linking it to the SWE variation. Their muon measurements agree with neutronic detector measurements and also with manual observations. We exploited the simulation potential and the control of laboratory samples to identify the actual SWE, and quantify its correlation with muon deviations. The fact of measuring deviation (MSR) instead of absorption (MAR), gave us additional information of the physical phenomenons that muons undergo, adding information about the multiple scattering they suffer when traversing snow samples.

The application and testing of our technique in the field, together with further research and innovation of muon detection systems and reconstruction algorithms can lead to the implementation of an industrialised MSR method for SWE determination. Characteristics of muon radiation such as the penetrating power and innocuousness make MSR an appropriate technology for the real time SWE monitoring. This technique also provides information about the density and composition of the target, allowing to identify material properties (Åström et al.,

2016), as well as internal density distributions (Vanini et al., 2019). These potentialities could eventually lead to retrieval of the internal layered structure of the snowpack. Locating and estimating the characteristics of the produced muon deviations through their trajectories and applying advanced muography algorithms (Schultz et al., 2007) (Sehgal et al., 2020) the snowpack density distribution could be estimated and voids or weak layers identified. The results of our proof of concept will be useful for the development of new sensors and detection algorithms, providing the necessary background for the future operational design of muon scattering based SWE monitoring networks.

## Acknowledgments

We highly appreciate the support of the Spanish Ministry of Science and Innovation. This ministry has funded the work of Aitor Orio-Alonso through the program “Ayudas para contratos para la formación de doctores en empresas (Doctorados Industriales) 2018” (Reference: DIN2018-009886). Esteban Alonso-González was supported by the postdoctoral grant of the Centre National d’Etudes Spatiales (CNES).

We also esteem the funding and support of the project of Muon Systems by Centro para el Desarrollo Tecnológico Industrial (CDTI) and the Government of the Basque Country.

## Open Research

The simulation and laboratory measurement snowpack and muon deviation data which is analysed in this paper is available in (Orio-Alonso et al., 2023) [Creative Commons Attribution International 4.0].

## References

- Agostinelli, S., Allison, J., Amako, K., Apostolakis, J., Araujo, H., Arce, P., Asai, M., Axen, D., Banerjee, S., Barrand, G., Behner, F., Bellagamba, L., Boudreau, J., Broglia, L., Brunengo, A., Burkhardt, H., Chauvie, S., Chuma, J., Chytrcek, R., ... Zschesche, D. (2003). GEANT4—A simulation toolkit. *Nuclear Instruments and Methods in Physics Research, Section A: Accelerators, Spectrometers, Detectors and Associated Equipment*, 506(3), 250-303. [https://doi.org/10.1016/S0168-9002\(03\)01368-8](https://doi.org/10.1016/S0168-9002(03)01368-8)
- Alonso-González, E., López-Moreno, J. I., Gascoin, S., García-Valdecasas Ojeda, M., Sanmiguel-Valladolid, A., Navarro-Serrano, F., Revuelto, J., Ceballos, A., Esteban-Parra, M. J., & Essery, R. (2018). Daily gridded datasets of snow depth and snow water equivalent for the Iberian Peninsula from 1980 to 2014. *Earth*

- System Science Data*, 10(1), 303-315. <https://doi.org/10.5194/essd-10-303-2018>
- Åström, E., Bonomi, G., Calliari, I., Calvini, P., Checchia, P., Donzella, A., Faraci, E., Forsberg, F., Gonella, F., Hu, X., Klinger, J., Ödqvist, L. S., Pagano, D., Rigoni, A., Ramous, E., Urbani, M., Vanini, S., Zenoni, A., & Zumerle, G. (2016). Precision measurements of Linear Scattering Density using Muon Tomography. *Journal of Instrumentation*, 11. <https://doi.org/10.1088/1748-0221/11/07/P07010>
- Barnett, T. P., Adam, J. C., & Lettenmaier, D. P. (2005). Potential impacts of a warming climate on water availability in snow-dominated regions. *Nature*, 438(7066), 303-309. <https://doi.org/10.1038/nature04141>
- Bartelt, P., & Lehning, M. (2002). A physical SNOWPACK model for the Swiss avalanche warning Part I: Numerical model. *Cold Regions Science and Technology*, 35(3). [https://doi.org/10.1016/S0165-232X\(02\)00074-5](https://doi.org/10.1016/S0165-232X(02)00074-5)
- Bethe, H. A. (1953). Molière's Theory of Multiple Scattering. *Physical Review*, 89(6), 1256. <https://doi.org/10.1103/PhysRev.89.1256>
- Bonechi, L., D'Alessandro, R., & Giammanco, A. (2020). Atmospheric muons as an imaging tool. *Reviews in Physics*, 5. <https://doi.org/10.1016/j.revip.2020.100038>
- Gugerli, R., Desilets, D., & Salzmann, N. (2021). *Brief communication: Application of a muonic cosmic ray snow gauge to monitor the snow water equivalent on alpine glaciers*. <https://doi.org/10.5194/tc-2021-277>
- Günther, D., Marke, T., Essery, R., & Strasser, U. (2019). Uncertainties in Snowpack Simulations—Assessing the Impact of Model Structure, Parameter Choice, and Forcing Data Error on Point-Scale Energy Balance Snow Model Performance. *Water Resources Research*, 55(4), 2779-2800. <https://doi.org/10.1029/2018WR023403>
- Hagmann, C., Lange, D., & Wright, D. (2012). Cosmic-ray shower generator (CRY) for Monte Carlo transport codes. *2007 IEEE Nuclear Science Symposium Conference Record*. <https://doi.org/10.1109/NSSMIC.2007.4437209>
- Highland, V. L. (1975). Some practical remarks on multiple scattering. *Nuclear Instruments and Methods*, 129(2), 497-499. [https://doi.org/10.1016/0029-554X\(75\)90743-0](https://doi.org/10.1016/0029-554X(75)90743-0)
- Jitnikovitch, A., Marsh, P., Walker, B., & Desilets, D. (2021). Snow water equivalent measurement in the Arctic based on cosmic ray neutron attenuation. *The Cryosphere*, 15(11), 5227-5239. <https://doi.org/10.5194/tc-15-5227-2021>

- 440 Lehning, M., Bartelt, P., Brown, B., & Fierz, C. (2002). A physical SNOWPACK model for the Swiss avalanche  
441 warning Part III: Meteorological forcing, thin layer formation and evaluation. *Cold Regions Science and  
442 Technology*, 35(3). [https://doi.org/10.1016/S0165-232X\(02\)00072-1](https://doi.org/10.1016/S0165-232X(02)00072-1)
- 443 Lehning, M., Bartelt, P., Brown, B., Fierz, C., & Satyawali, P. (2002). A physical SNOWPACK model for the Swiss  
444 avalanche warning Part II. Snow microstructure. *Cold Regions Science and Technology*, 35(3).  
445 [https://doi.org/10.1016/S0165-232X\(02\)00073-3](https://doi.org/10.1016/S0165-232X(02)00073-3)
- 446 Luojus, K., Pulliainen, J., Takala, M., Lemmetyinen, J., Mortimer, C., Derksen, C., Mudryk, L., Moisander, M.,  
447 Hiltunen, M., Smolander, T., Ikonen, J., Cohen, J., Salminen, M., Norberg, J., Veijola, K., & Venäläinen, P.  
448 (2021). GlobSnow v3.0 Northern Hemisphere snow water equivalent dataset. *Scientific Data*, 8(1), 163.  
449 <https://doi.org/10.1038/s41597-021-00939-2>
- 450 Lynch, G. R., & Dahl, O. I. (1991). Approximations to multiple Coulomb scattering. *Nuclear Instruments and  
451 Methods in Physics Research Section B: Beam Interactions with Materials and Atoms*, 58(1), 6-10.  
452 [https://doi.org/10.1016/0168-583X\(91\)95671-Y](https://doi.org/10.1016/0168-583X(91)95671-Y)
- 453 Martínez-Ruiz del Árbol, P., Gómez-García, P., Díez-González, C. D., & Orio-Alonso, A. (2018). Non-destructive  
454 testing of industrial equipment using muon radiography. *Philosophical transactions. Series A,  
455 Mathematical, physical, and engineering sciences*, 377(2137). <https://doi.org/10.1098/rsta.2018.0054>
- 456 Martínez-Ruiz del Árbol, P., Orio-Alonso, A., Díez-González, C., & Gómez-García, P. (2022). Applications of  
457 Muography to the Industrial Sector. *Journal of Advanced Instrumentation in Science*.  
458 <https://doi.org/10.31526/jais.2022.267>
- 459 Moreno, J. I. L., Quirós, B. A., Latron, J., & Fassnacht, S. R. (2010). Instalación y uso de un colchón de nieve para  
460 la monitorización del manto de nieve. Cuenca Experimental de Izas (Pirineo Central). *Cuadernos de  
461 investigación geográfica: Geographical Research Letters*, 36, 73-82.
- 462 Mori, N., Ambrosino, F., Bonechi, L., Cimmino, L., D'alessandro, R., Noli, P., Saracino, G., Strolin, P., & Viliani,  
463 L. (2017). A geant4 framework for generic simulations of atmospheric muon detection experiments. *Annals  
464 of Geophysics*, 60(1). <https://doi.org/10.4401/AG-7383>
- 465 Muñoz-Sabater, J., Dutra, E., Agustí-Panareda, A., Albergel, C., Arduini, G., Balsamo, G., Boussetta, S., Choulga,  
466 M., Harrigan, S., Hersbach, H., Martens, B., Miralles, D. G., Piles, M., Rodríguez-Fernández, N. J., Zsoter,  
467 E., Buontempo, C., & Thépaut, J.-N. (2021). ERA5-Land: A state-of-the-art global reanalysis dataset for

- land applications. *Earth System Science Data*, 13(9), 4349-4383. <https://doi.org/10.5194/essd-13-4349-2021>
- Orio-Alonso, A., Alonso-González, E., Martínez-Ruiz del Árbol, P., Díez-González, C., & Gómez-García, P. (2023). *Snowpack simulation and Muon Scattering Radiography (MSR) measurements*. <https://doi.org/10.5281/zenodo.7547306>
- Raleigh, M. S., Livneh, B., Lapo, K., & Lundquist, J. D. (2016). How Does Availability of Meteorological Forcing Data Impact Physically Based Snowpack Simulations? *Journal of Hydrometeorology*, 17(1), 99-120. <https://doi.org/10.1175/JHM-D-14-0235.1>
- Revuelto, J., López-Moreno, J. I., & Alonso-González, E. (2021). Light and Shadow in Mapping Alpine Snowpack With Unmanned Aerial Vehicles in the Absence of Ground Control Points. *Water Resources Research*, 57(6), e2020WR028980. <https://doi.org/10.1029/2020WR028980>
- Schultz, L. J., Blanpied, G. S., Borozdin, K. N., Fraser, A. M., Hengartner, N. W., Klimenko, A. V., Morris, C. L., Orum, C., & Sossong, M. J. (2007). Statistical reconstruction for cosmic ray muon tomography. *IEEE Transactions on Image Processing*. <https://doi.org/10.1109/TIP.2007.901239>
- Sehgal, R., Mitra, M. S., Roy, T., Sehgal, S. T., Pant, L. M., & Nayak, B. K. (2020). Voxelization based PoCA point cloud filtration algorithm for image reconstruction for Muon Tomography. *Journal of Instrumentation*, 15(9). <https://doi.org/10.1088/1748-0221/15/09/P09012>
- Vanini, S., Calvini, P., Checchia, P., Garola, A. R., Klinger, J., Zumerle, G., Bonomi, G., Donzella, A., & Zenoni, A. (2019). Muography of different structures using muon scattering and absorption algorithms. *Philosophical Transactions of the Royal Society A: Mathematical, Physical and Engineering Sciences*, 377(2137). <https://doi.org/10.1098/RSTA.2018.0051>
- Vionnet, V., Marsh, C. B., Menounos, B., Gascoin, S., Wayand, N. E., Shea, J., Mukherjee, K., & Pomeroy, J. W. (2021). Multi-scale snowdrift-permitting modelling of mountain snowpack. *The Cryosphere*, 15(2), 743-769. <https://doi.org/10.5194/tc-15-743-2021>
- Workman et al. (Particle Data Group), R. L. (2022). Review of Particle Physics. *Prog. Theor. Exp. Phys.* 2022, 083C01, 34. *Passage of Particles Through Matter*. <https://doi.org/10.1093/ptep/ptac097>
- Zeng, W., Zeng, M., Pan, X., Zeng, Z., Ma, H., & Cheng, J. (2020). Principle study of image reconstruction algorithms in muon tomography. *Journal of Instrumentation*, 15(2). <https://doi.org/10.1088/1748->

496 0221/15/02/T02005

497

498

499